Characterization of Tensile Properties of Woven Ceramic Composites at Room and Elevated Temperature

Mehran Elahi
Elizabeth City State University
melahi@mail.ecsu.edu

Abstract

Materials development holds the key for the United States to maintain or even increase its share of the world engine market. One of the major contributors to this goal is the development of advanced engineering materials for engines that will be used as the propulsion system for subsonic and supersonic commercial aircraft.

The goal of this investigation is to characterize durability of a model ceramic composite material at room and elevated temperatures. The material of choice is silicon carbide fiber (Nicalon[1]) reinforced silicon carbide matrix enhanced composite processed by a chemical vapor infiltration technique. In this paper design and development of a computer controlled elevated temperature (≥1800 ^oF) fully aligned testing system and testing methodology with capability to carry out long-term dynamic (high cycle fatigue) tests is discussed. Also results of room and elevated temperature quasi-static tensile tests for various stacking sequence and the effect of a notch are presented. Thermomechanical behavior as well as potential damage modes and failure mechanisms as a function of stacking sequence, specimen geometry, and testing temperature are discussed.

1.0 Introduction

This paper reports the findings from the first phase of a comprehensive experimental investigation to characterize durability of a model ceramic matrix composite material (CMC) intended for high temperature applications. In this phase of the investigation a comprehensive literature survey was conduced, and a high temperature material testing system was designed and developed. Finally mechanical tests were conducted to obtain material properties at room and elevated temperature where these results will be used as the baseline data for future durability (cyclic fatigue) tests.

For the past couple of decades there has been a concerted effort to develop the technology required to build a high-speed civil transport aircraft (HSCT) that is capable of flying at speeds as high as Mach 3.5. Flying at these speeds in a commercial/ civilian environment demands addressing economics and environmental issues. The later is translated into two engine components design considerations. First, to design a combustor with lower levels of nitrous oxide (NOx) emission than the current levels, and second, to design a light-weight exhaust nozzle that meets the federal aviation agency (FAA) regulation on community

ISBN 978-1-60643-379-9

noise standards. The effort to design and develop the combustor material, which meets the required environmental, economic, thermal, structural, and durability standards (18000 hr life), was initiated under the enabling propulsion material program [1].

With the exception of a few materials, most ceramics appear to be marginal for use in jet engines at elevated temperatures. At low temperatures, the brittle fracture of monolithic ceramic materials is related to pre-existing flaws and defects which may have been induced during the fabrication process. These flaws serve as the nucleation sites for cracks which can grow under load and propagate to a critical size resulting in fracture. Because there is typically a distribution of such flaws, there is a resulting scatter in material strength also. Monolithic ceramics are linearly elastic, and their strength is controlled by the largest flaw present in the tested volume. These materials can exhibit the phenomenon of slow (subcritical) crack growth under load at high temperatures, suggesting that the strength is time dependent. Above 1800 °F, these materials are statically unstable and show creep deformation [2, 3].

To achieve satisfactory levels of strength, fracture toughness, and reliability, fiber reinforced composites will be required [4]. Reinforcement of ceramic matrix materials with high modulus and high strength continuous ceramic fibers results in tougher materials with superior fatigue, creep, and thermal shock resistance [5]. The strength properties do not depend on the largest pre-existing flaw formed during fabrication; but rather, depend on the complex interaction of local stress field around the flaws and their growth due to global stresses [3].

The use of continuous fiber reinforced CMCs for propulsion applications (such as the next generation of commercial supersonic aircraft) requires performance and durability evaluation of these materials under static and dynamic loading at elevated temperatures (≥1800 °F).

Now there is great demand for information regarding long-term deformation characteristic of CMCs such as fatigue and creep. To identify potential damage modes and failure mechanisms in ceramic and glass-ceramic composites due to mechanical and thermal as well as environmental effects a comprehensive literature survey was conducted by the author [6]. The material evaluation and analysis obtained from the literature survey indicates that the properties of silicon carbide/silicon carbide composites are most promising for combustor liners. This study is intended to characterize the thermomechanical behavior of a model material.

The material of choice is silicon carbide fiber (Nicalon[1]) reinforced enhanced silicon carbide matrix composite processed by a chemical vapor infiltration (CVI) technique. This material system is simply referred to as Nicalon[1]/E-SiC. To better understand the material behavior under various testing conditions the processes involved in production of Nicalon[1] fibers and the Nicalon[1]/SiC composites are described in the following few paragraphs.

Fiber and Material Processing

Continuous ceramic fibers have become very attractive as a reinforcing material because of their superior strength, elastic modulus and high-temperature capabilities. There are various methods of fabricating ceramic fibers, which may be categorized as polymer pyrolysis, chemical vapor deposition (CVD), and sol-gel techniques [7]. The first two methods are used in production of SiC fibers. To get an insight into the nature and microstructure of Nicalon[1] fibers, the following paragraph explains the manufacturing process involved in production of Nicalon[1] fibers via polymer pyrolysis technique [7].

Production of ceramic fibers via polymer pyrolysis process is considered to be a great breakthrough in development of ceramic fibers. This process traditionally has been used to produce carbon fibers from carbon-based polymers. However demand for materials with better thermal stability, higher oxidation resistance and superior mechanical properties has resulted in production of ceramic fibers and coatings such as B_4C, BN, SiC and Si_3N_4 from polymers containing C, B, Si, and N_2 under very controlled conditions. Nicalon[1] fiber is one of those ceramic fibers that were developed through polymer pyrolysis.

Ceramic composite processing via CVI technique has gained a lot of attention in the past few years. This processing method is one of the few processes, which is known not to damage fibers chemically, thermally or mechanically upon processing and provides the capability to produce near net shape composites. In general, a CVI processing system is composed of reactor in which the fiber preform is held at high temperatures inside a furnace. Then the reactant gases are entered into the furnace and are passed through the preform, which upon exposure to high temperature react and a layer of solid coating gets deposited on the fibers. As this process continues the fiber coating gets larger and finally interlocks with the neighboring fiber coatings causing fibers to hold together in form of a bundle [8].

Material Behavior

Nicalon[1]/SiC composites have shown different behavior depending on the testing temperature, atmospheric condition, and test duration. Tensile or flexural response of these materials is represented by stress-strain (load-deflection) curves which indicate linear elastic behavior up to a point where the proportional limit strength (PLS) is very much saturated by matrix cracking. Further loading initiates further matrix microcracking and partial fiber-matrix debonding, resulting in a nonlinear region which is probably controlled by fiber pull-out, crack deflection, and fiber bridging mechanisms [9, 10].

The performance of continuous fiber reinforced ceramic matrix composites is significantly influenced by processing techniques and processing parameters as well as fiber architecture [11, 12]. In cases where woven fiber preform is used, the matrix is introduced by infiltration or deposition techniques. Stress-strain behavior is directly related to the degree of infiltration and porosity created due to the differences in the infiltration processes. Fiber architecture will not only affect the infiltration of the matrix, but also the mechanical porosity and failure behavior by influencing the pore size, pore geometry, and pore distribution of the fibrous preform. These pores act as points of crack initiation and the strength decreases significantly as the void fraction increases [13, 14].

Thermal exposure results in fiber strength degradation. Nicalon[1] fibers are found to lose strength above 1832 °F, which in turn can result in modification of the fiber-matrix interface [15, 16]. Also it is reported that Nicalon[1] fiber is susceptible to decomposition, oxidation, accelerated grain boundary growth, and creep at elevated temperatures. Exposing Nicalon[1] fibers at elevated temperatures in an oxidizing environment for a long period of time causes the crystallization of the amorphous silica layer which is associated with volume decrease [17, 18, 19].

An oxidizing environment is found to have a detrimental effect on the fracture behavior of unprotected specimens; i.e., fiber pullout and toughness. These effects are reported to be progressive. Oxidation at 1832 °F for a short period of time results in a loss of ultimate strength and PLS; however, the failure of these composites is associated with significant fiber pullout. As the exposure time increases, the degree of fiber pullout decreases, which ultimately results in brittle fracture [20]. This progressive weakening and embrittlement of the material is believed to be the direct result of removal of the initial carbon interface and growth of a silica layer. This fiber-matrix interface evolution causes a strong and brittle bond between the fibers and the matrix.

2.0 Investigative Approach

To understand mechanical behavior of advanced ceramic composites, one needs to experimentally observe and measure the long-term behavior and predict the remaining strength and life under the service environment of the actual engineering component. To fulfill these goals the following objectives were established for this and future investigations.

- To design and develop a fully aligned computer controlled material testing system with long term (cyclic) elevated temperature testing capability and a testing methodology up to 2200 ^{o}F To characterize tensile material mechanical properties at 75 ^{o}F and 1832 ^{o}F
- To characterize the notch effect on tensile material properties at 75 ^{o}F and 1800 ^{o}F
- To investigate notch effect on stress distribution and local elastic properties
- To investigate the influence of specimen geometry, stacking sequence, load level, and loading type on remaining strength and other related mechanical properties
- To investigate NDE techniques to evaluate the damage mode and failure mechanisms

The details of the last three tasks will be provided in future publications.

Material System, Stacking Sequence, Notch Effect, Specimen Geometry

In this investigation 2-D woven flat coupons made of Nicalon/E-SiC composite were chosen as test specimens. The material was processed by an isothermal chemical vapor infiltration (ICVI) technique and is manufactured by DuPont Lanxide Composites Inc based in Delaware, USA. The fiber is of ceramic grade Nicalon[1], 1800 denier, 500 filaments per tow, balanced plain weave cloth (0/90 plain weave cloth), with 17 tows per inch and cloth areal weight of 8.24 oz/yd^2. The matrix material is SiC containing boron-based particles for protection of fibers against oxidation (thus enhanced with respect to previous version). Each ply has a thickness of 0.0105″, density of 0.83 lbs/in^3, fiber volume fraction of 40%, and porosity of 12%. The enhanced version is developed based on the same manufacturing techniques as with the original Nicalon[1]/SiC and is believed to have superior stress rupture behavior [21]. The final product is in form of square panels (12″×12″).

For this study the coupons were cut from the panels and were put back into the furnace where a layer of SiC (80-100 μm) was chemically vapor deposited on their outer surface for further protection against oxidation. Bow-tie shaped specimens with stacking sequences of $[(0,90)/(0,90)]_{2s}$ (cross-ply) and $[(0,90)/(+45,-45)]_{2s}$ (quasi-isotropic) were chosen for this phase of investigation. Due to the limited availability of test specimens only one cross ply specimen was dedicated to room temperature testing. This test was useful in verifying material behavior as reported by the manufacturer, and in checking the existing testing system and material system. This data could always be complemented by the room temperature data provided by material manufacturer. The other three specimens were tested at 1800 °F. The quasi-isotropic specimens were evenly distributed for each test temperature. Quasi-static tensile test matrix of unnotched cross-ply and unnotched quasi-isotropic laminates are presented in Table 1.

Table 1: Test matrix for $[(0,90)/(0,90)]_{2s}$ and $[(0,90)/(+45,-45)]_{2s}$ laminates.

No. of Tests	Stacking Sequence	Loading Mode	Atmosphere	Test Temp. (°F)
1	$[(0,90)/(0,90)]_{2s}$	Stroke	air	74
3	$[(0,90)/(0,90)]_{2s}$	Stroke	air	1800
2	$[(0,90)/(+45,-45)]_{2s}$	Stroke	air	74
2	$[(0,90)/(+45,-45)]_{2s}$	Stroke	air	1800

Furthermore, notched specimens were tensile tested to study influence of notches on material response, damage initiation, damage growth and state stress in the material. Notch effect on material response was investigated by testing quasi-static tensile tests at 75 °F and 1800 °F in air. The results were examined and compared to the corresponding unnotched specimens. Effect of notch on state of stress in the material was investigated by application of strip strain gages around at the hole and conducting room temperature tensile tests. Room temperature material response at incremental distances from the hole was recorded upon application of load. Table 2 lists the complete test matrix for the notched specimens. A detailed account of notch effect investigation will be provided in a future publication.

Table 2: Test matrix for center notched $[(0,90)/(0,90)]_{2s}$ laminates.

No. of Tests	Type of Test	Loading Mode	Test Temp. (°F)	Atmosphere
2	Quasi-Static Tensile	Stroke	75	air
2	Quasi-Static Tensile	Stroke	1800	air
1	Strip Gage	Load	75	air

Specimen Geometry

Based on the above test matrices, two types of specimen geometries were selected, notched and unnotched. The unnotched specimens were cut in a bow-tie shape from the panels with cross-ply and quasi-isotropic stacking sequences. Based on their width, they were further divided into two categories. The wide specimens with an average thickness of 0.09″, gage section width of 0.75″, grip section width of 0.85″, and length of 6.0″, and the narrow ones with an average thickness of 0.09″, gage section width of 0.40”, grip section width of 0.50″, and length of 6.0″. The notched specimens were cut from the $[(0,90)/(0,90)]_{2s}$ panels in a straight edge rectangular shape. They were measured to have an average thickness of 0.09″, width of 1.50″, and a length of 6.0″ with a 0.25″ diameter hole drilled through at their geometric center (Figure 1).

Specimen thickness and width numbers represent average values of three measurements that were made inside the one-inch extensometer gage length located at the center of the specimen. Visual inspection of specimens indicated large variations on surface uniformity and texture. These were mainly due to presence of patches of excess seal coating material on the surface of specimens. These variations were found to be a function of panel numbers, which may be explained by the fact that the panels were processed at different times. It is believed that the excess CVD of SiC layer on the outside surface of each panel created this non-uniformity. All the specimens were inspected using x-ray radiograph prior to any mechanical or thermal testing (Figure 1).

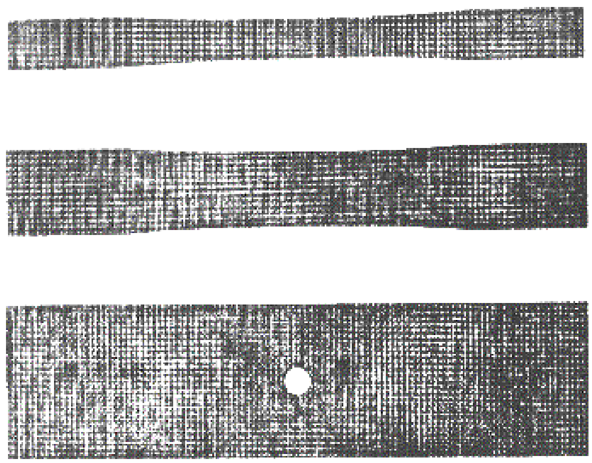

Figure 1: X-ray radiographs of the test specimens.

3.0 Results and Discussions

With mechanical testing of high temperature materials such as ceramic matrix composites many factors such as load train, load train alignment, gripping, heating system and heating process, and strain measurement process and device can influence the test results. To be able to characterize long-term mechanical behavior of CMCs under in-service environment, an axial testing system with high temperature testing capability was developed. The testing system included a hydraulic testing frame, a furnace, cooling system, an extensometer with high temperature application, and a data acquisition/controller computer system (Figure 2). This system can be used for long-term mechanical tests such as creep and high cycle fatigue for temperatures up to 2200 °F. The various parts of this test system along with the related issues are briefly explained in the following paragraphs.

High Temperature Testing System

Mechanical tests were performed by a servo controlled; hydraulically actuated, Material Testing Systems (MTS) load frame with a load capacity of 22 kips. Since ceramic matrix composites generally exhibit failure to strains of less than 1.5%, machine misalignment also becomes one of the primary concerns in any quasi-static or cyclic testing where small amounts of bending could cause premature matrix cracking and influencing the material response. The alignment of testing frame was determined per HSCT standards [22]. The alignment instrument used in this study was a rectangular shaped accurately ground steel bar. The bar was equipped with four resistance foil strain gages at perpendicular planes on either side of the bar's mid-section (total of 8 gages). Test system exhibited a maximum bending strain (face to face) of 12.5 micro strain upon gripping the specimen at zero applied load and a maximum bending of 7.8% at each plane (face to face and edge to edge) for an applied load of 1000 pounds.

Due to versatility and ease of use, a cold gripping system was employed. This system utilized two sets of water-cooled hydraulic wedge grips, which were essential for through-zero loading of the flat coupon-type specimens. The recent finding has shown that acceptable temperature gradients can be achieved with this technique up to 4200 °F [23].

In all the tests flat friction loaded specimens were gripped using three layers of 60 aluminum grid sand paper under a grip line pressure of 400-450 psi. Due to size of the furnace and the need to insulate the furnace with high temperature insulation blanket, only one inch at each ends of a 6″ long specimen was gripped. Measurement showed that for a test temperature of 1832 °F the upper grip temperature did not exceed a maximum of 170 °F. The cooling of the whole system was achieved by sending cold water through hydraulic wedge grips, high temperature extensometer, and extensometer heat shield. The cooling system included a solenoid valve, water filter, inlet flow meter and outlet flow meter. These features were included in the cooling network so that in future the cooling process could be monitored via a computer controlled environment. The system safety net was designed so that the heating process and water pressure could be terminated upon triggering the alarms which were to be set based on inlet water flow, inlet and outlet flow differential, grip temperature, furnace temperature, load level, and operation of hydraulic testing frame. These features are necessary in any long-term elevated temperature testing (Figure 2).

A convection/radiation heating method was used via a splitting face, box type furnace (3.25″×3.25″×3.25″) with a series of heating elements. In process of setting up the heating system, which included numerous dry run tests to further smooth the heating process, few observations were made. Originally, furnace was equipped with three sets of heating elements (three on each side). But it was learned (by trial and error) for better temperature control, the middle heating elements should not make any contribution therefore they were disconnected (not removed). The furnace operation was controlled by a microprocessor-based temperature and process controller (master and slave type) via monitoring the specimen temperature using two R-type thermocouples positioned 2.5″ apart on the thickness side of the specimen. Also, for optimum temperature control, the master controller had to be connected to thermocouple closest to the top heating elements and the slave controller to the thermocouple closest to the bottom heating elements. The smooth operation of extensometer was best achieved when the power outputs (not the temperature) by the master and slave controllers were reasonably stable (not necessarily equal). This may be explained by the fact that thermocouples have slower response than extensometers.

The heating process was accomplished according to HSCT standards [23], which required monotonically increasing the test temperature to the target value within a period of 15-20 minutes. Reaching a test temperature of 1800 °F in 20 minutes requires a heating rate of 90 °F per minute. Achieving this heating rate, overall operation of the furnace and ultimately specimen temperature profile were influenced greatly by how well the heating system was insulated. Except for the access ports for extensometer rods (two 0.25″ dia holes), thermocouples (three 0.2″ dia. holes), and the specimen (two 0.2″×1.5” slits in case of notched specimens), furnace was completely insulated by one-inch thick insulation blanket.

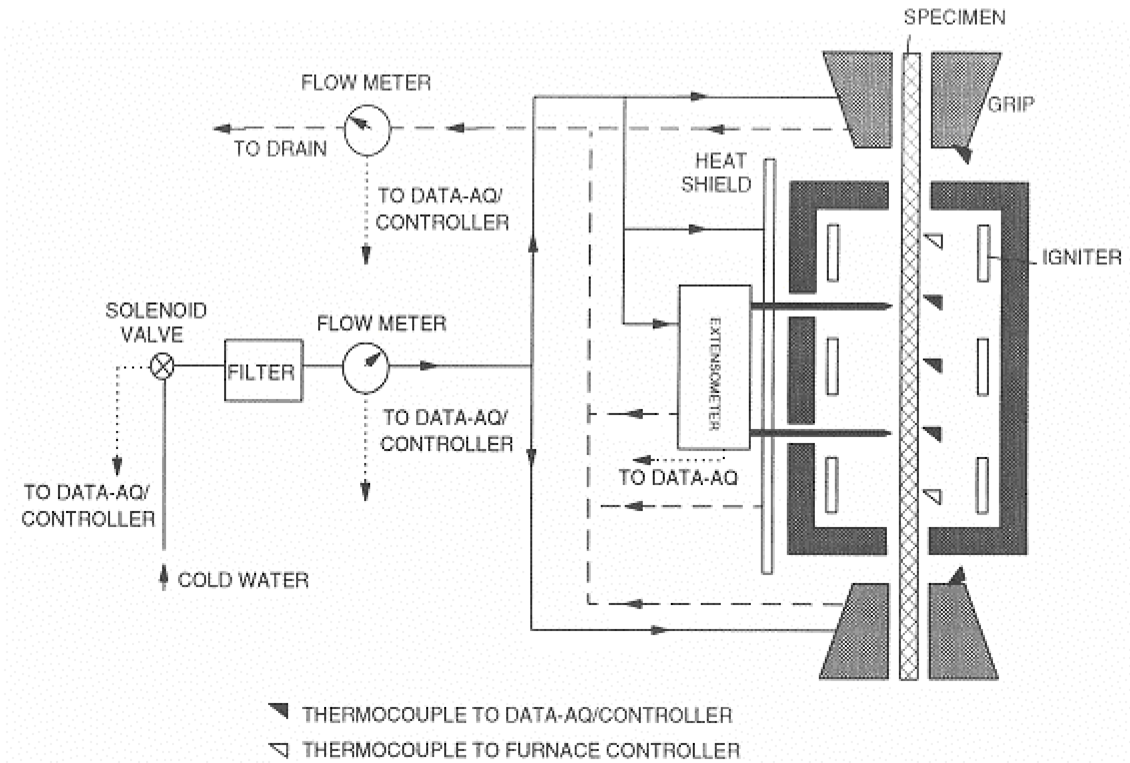

Figure 2: Schematic of the test set-up for elevated temperature axial testing.

This configuration guaranteed smooth operation of heating system for heating rate as high as 120 °F. Although the temperature overshoot did not exceed 1% for test temperature of 1832 °F, the heat up ramp was always followed by a 20 minutes soak time to further stabilize the specimen temperature prior to any load application (Figure 3).

The temperature uniformity of the test specimen was monitored by readings of five thermocouples inside the 2.0-inch gage section. One was placed at the middle of gage section followed by the rest of the thermocouples as two were placed, separated 0.5″ from each other, on either side of the middle section. Variations in test temperature along the length of specimen were less than 0.1% (Figure 4).

In elevated temperature testing, specimens were gripped and heated up to the desired temperature in load control mode. This mode of control prevented risk of any possible damage to the specimens, as a result of thermal expansion, prior to mechanical testing. For tensile testing, once the prescribed temperature was reached, control mode was switched from load to stroke. This was not possible with the controller 448 MTS controller and a 458 MTS controller was used instead. To be consistent in all of the tensile testing, same procedure was followed for room temperature testing also.

For room temperature strain measurements an extensometer with 1″ gage length with maximum operating temperature of 350 ^{o}F, 15% maximum range, and 1.5% calibrated operating range, was placed at the geometric center of the specimens. The knife edges of extensometer were securely placed via rubber bands. Elevated temperature strain measurement was made possible via a one-inch gage length MTS extensometer designed for high temperature applications (maximum operating temperature of 2200 ^{o}F) with 15% linear operating range capability.

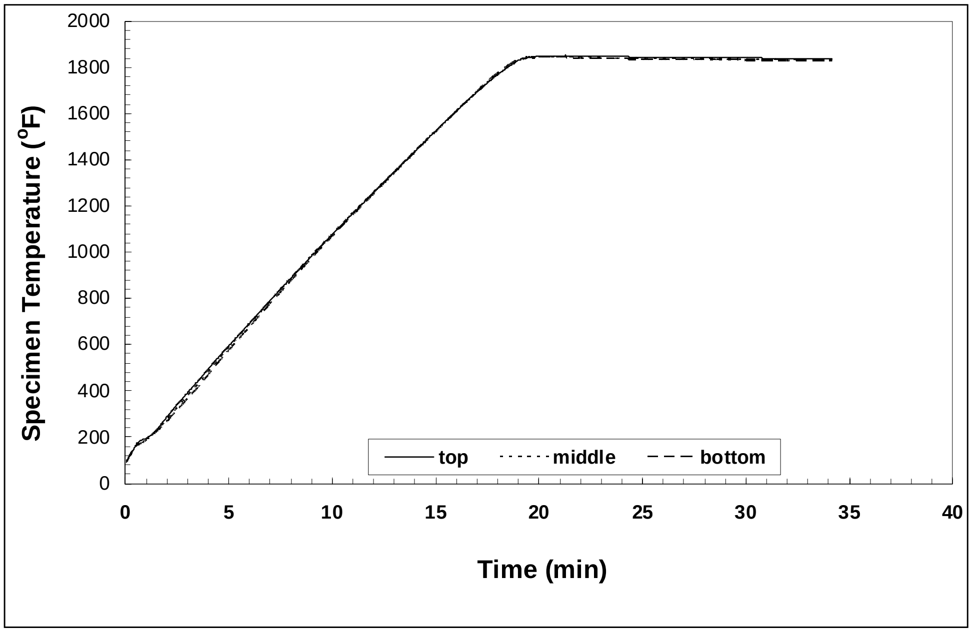

Figure 3: Typical heating cycle for elevated temperature testing.

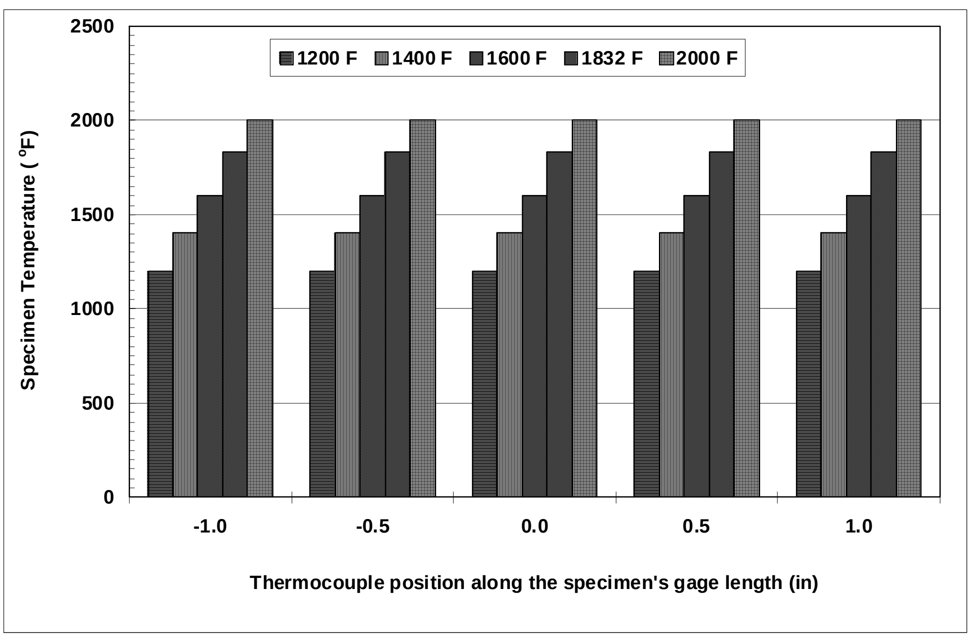

Figure 4: Specimen temperature profile for various furnace temperature settings.

In this investigation an extensometer, calibrated for 1.5%, range, was used. This is a water-cooled unit (requires certain water flow rate for maximum cooling and smooth operation), which comes in contact with specimen via two alumina rods (6″ long). Rods were loaded (0.25 pound) by the leaf springs mounted on the heat shield bracket. Due to surface roughness of specimens alumina rods with conical ends were used as opposed to the rods with straight knife-edge. Alumina rods with recommended maximum operating temperature of 2200 ^{o}F are the main limiting factor in using the extensometer unit at higher temperatures.

Quasi-Static Tensile Test

Room and elevated temperature (1800 °F) quasi-static tensile tests were conducted to evaluate tensile response, corresponding mechanical properties and the temperature effects on tensile behavior. Ultimately, these results will be used to define fatigue load limits and as the baseline data for comparison with remaining properties for various loading situations (future study). These tests were carried out according to the HSCT standards for quasi-static tensile testing of ceramic matrix composites [24]. This required monotonic tensile tests under stroke control for a pre determined stroke rate of 0.02 in/min (obtained by trial and error) in atmospheric air. Test results of unnotched $[(0,90)/(0,90)]_{2s}$ laminates, unnotched $[(0,90)/(+45,-45)]_{2s}$ laminates, and center-notched $[(0,90)/(0,90)]_{2s}$ laminates are presented in the following sections. Each table lists individual test results along with their average values.

Unnotched $[(0,90)/(0,90)]_{2s}$ Laminates

A total of four specimens, one at 75 °F and three at 1800 °F, were pulled to failure quasi-statically. Typical tensile responses are presented in Figure 5. Stress-strain curves indicate typical response of fiber reinforced ceramic matrix composites in which upon application of load, material deforms elastically in linear manner with a Young's elastic modulus of Ei. This region although linear but it is associated with some micro cracks, fiber matrix debonding and fiber breaks. This regime extends up to the start of a second region, which is highly nonlinear. In this region the existing matrix micro cracks transform into major cracks causing large amount of fiber breaks and subsequent fiber pullouts which bridge the cracks. The stress associated with this region marks a definite transition from the linear elastic region to a nonlinear region, is referred to as the Proportional Limit Strength (PLS). Following the HSCT standards [24], this point was obtained by locating the point of intersection between the stress-strain curve and a line drawn parallel to slope of initial Young's elastic modulus with 0.005% offset strain. Following this transition region, further application of load causes appearance of a second region (nonlinear), which is associated with large amount of fiber breaks, fiber pull-out and fiber bridging. In this region fibers are the main load carriers. More loading causes statistically enough fiber breakage in which the material cannot sustain any further loading resulting in failure of the specimen. This point marks the Ultimate Tensile Strength (UTS) of the material.

Measured material properties for both test temperatures are presented in Table 3. From room temperature responses, average values of 22.0 Msi for Ei, 29.5 ksi for UTS and strain to failure of 0.32% were obtained. The PLS was measured to be 12.3 ksi with a corresponding strain of 0.06%. It should be noted that in the DuPont Lanxide data, the PLS of 8.0 ksi with a corresponding strain of 0.045%, was not measured with any offset strain. This may explain the lower PLS value reported by DuPont Lanxide. In general, the obtained UTS and strain to failure data were significantly lower than the DuPont Lanxide data. Based on the fracture location, the 1800 ^{o}F test results have shown large variations for material

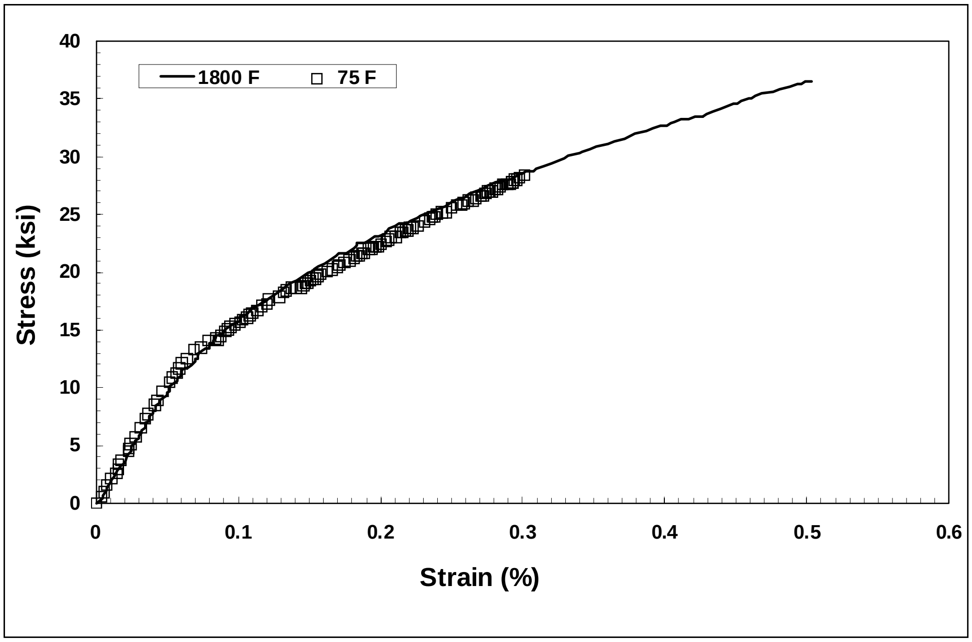

Figure 5: Room and elevated temperature tensile responses of $[(0,90)/(0,90)]_{2s}$ laminates.

response especially in strain to failure values. Therefore, it was decided to use tests results with highest strain to failure values (specimens i.d.'s 007-01-022-03 and 0007-001-025-03) for averaging purposes. This resulted in average values of 20.5 Msi for Ei, 35.8 ksi for UTS, and 0.52% for strain to failure, 12.35 ksi for PLS, and 0.07% for its corresponding strain.

Table 3: Quasi-static tensile test♣ results of $[(0,90)/(0,90)]_{2s}$ laminates.

Specimen I.D.	Gage Width (in)	Test Temp. (^oF)	Elastic Modulus Ei (Msi)	PLS Stress @ 0.005% Offset (ksi)	PLS Strain @ 0.005% offset (%)	Ultimate Strength UTS (ksi)	Ultimate Strain (%)	Fracture Location
007-01-017-02	0.75	74	22.00	12.30	0.060	29.50	0.320	OX
Ave. Value	***-----***	***74***	***22.00***	***12.30***	***0.060***	***29.50***	***0.320***	***-----***
Du Pont∗	***-----***	***73***	***20.50***	***8.00***	***0.045***	***33.00***	***0.410***	***-----***
007-01-018-04	0.75	1800	20.00	12.10	0.070	32.20	0.440	OX
007-01-022-03	0.40	1800	21.00	12.00	0.070	35.00	0.530	IX
007-01-025-03	0.40	1800	20.00	12.70	0.070	36.60	0.510	IX
Ave. Value	***----***	***1800***	***20.50***	***12.35***	***0.070***	***35.80***	***0.520***	***-----***

♣ Tests were performed at Cincinnati Testing Laboratory (CTL) for Pratt &Whitney.

∗ Ave. values of 81 room temperature tests performed by Du Pont Lanxide Composites, Inc.

The above test results have revealed significant temperature influence on material properties. On average the 1800 ^oF tests have resulted in a decrease of 7% in Ei, an increase of 21% and 62% in UTS and strain to failure respectively. The increase in ultimate stress and strain can be related to relaxation in residual stresses and ultimately disappearance of interface. Although the increase in PLS was not significant but its corresponding strain showed an increase of 16%. It is notable that for elevated temperature tests the specimens that failed inside the extensometer gage length (ix) show higher strain to failure values.

Unnotched $[(0,90)/(+45,-45)]_{2s}$ Laminates

A total of four specimens with $[(0,90)/(+45,-45)]_{2s}$ stacking sequence were equally distributed for 74 °F and 1800 °F tests. In general tensile responses were similar to the cross-ply case (Figure 6).

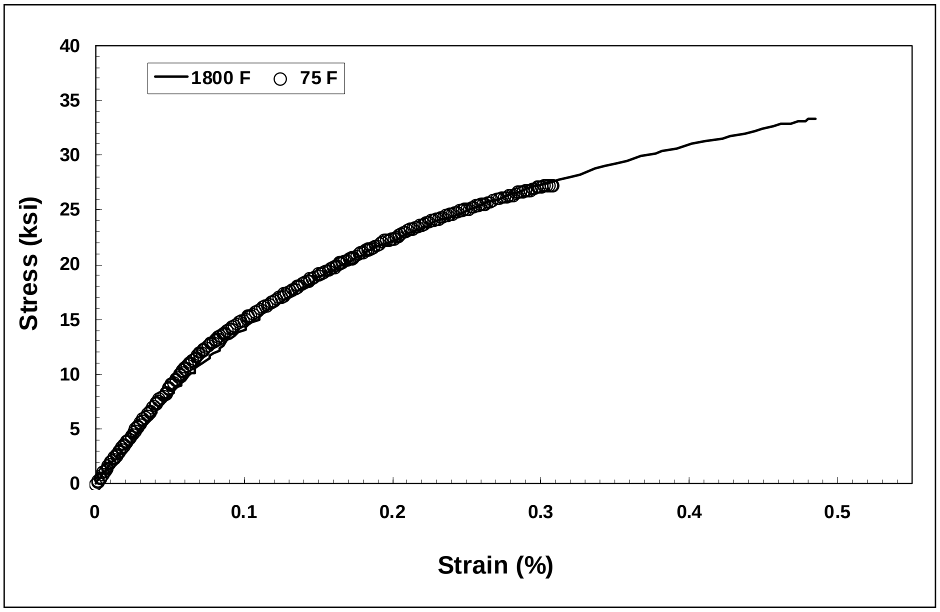

Figure 6: Room and elevated temperature tensile responses of $[(0,90)/(+45,-45)]_{2s}$ laminates.

Table 4: Quasi-static tensile test♣ results of $[(0,90)/(+45,-45)]_{2s}$ laminates.

Specimen I.D.	Gage Width (in)	Test Temp. (^{o}F)	Elastic Modulus Ei (Msi)	PLS Stress @ 0.005% offset (ksi)	PL Strain @ 0.005% offset (%)	Ultimate Strength (ksi)	Ultimate Strain (%)	Fracture Location
007-01-012-01	0.75	74	20.00	10.70	0.060	31.20	0.390	OX
007-01-012-07	0.75	74	18.0	12.00	0.070	27.50	0.310	OX
Ave. Value	***----***	***74***	***19.00***	***11.35***	***0.0650***	***29.35***	***0.350***	***-----***
007-01-012-02	0.75	1800	16.00	12.40	0.080	32.30	0.430	OX
007-01-012-04	0.75	1800	16.00	11.00	0.080	33.60	0.490	IX
Ave. Value	***----***	***1800***	***16.00***	***11.70***	***0.080***	***32.95***	***0.460***	***-----***

Room temperature tests resulted in average initial elastic modulus of 19.0 Msi, UTS of 29.35 ksi and strain to failure of 0.35%, PLS of 11.35 ksi with strain of 0.065% at PLS. Elevated temperature tests resulted in a decrease of 16% in Ei, an increase of 12% in UTS and an increase of 31% in strain to failure from their corresponding room temperature values. The PLS basically remained unchanged but the corresponding strain showed an increase of 23%. In comparison to cross-ply laminates, most of the room temperature properties of quasi-isotropic laminates remained the same except for elastic modulus, which showed a drop of 14%. The influence of off-axis lamination on material properties was more obvious for 1800 °F tests. A decrease of 22%, 8% and 12% for Ei, UTS and strain to failure were recorded respectively. The change in PLS was not significant but its strain decreased by 14%.

Center-Notched $[(0,90)/(0,90)]_{2s}$ Laminates

Room and elevated temperatures tensile tests of center notched cross-ply laminates were conducted by measuring the strain across the hole in direction of load application.

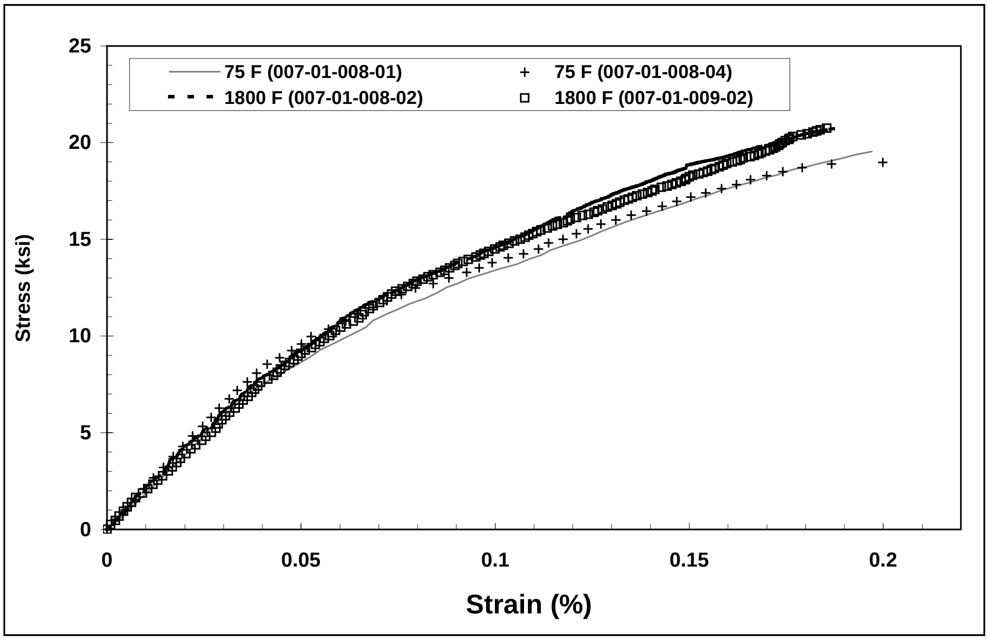

Figure 7: Room and elevated temp. tensile responses of notched $[(0,90)/(0,90)]_2s$ laminates.

Stress-strain responses and material properties for both test temperatures are presented in Figure 7 and Table 5 respectively. Notch influence preceded the temperature effect therefore resulting in similar mechanical properties for both temperatures. The notch influenced the 75 ^{o}F tests by decreasing UTS and strain to failure by 35% and 38% from their corresponding unnotched values. As expected, initial elastic modulus remained basically unchanged at 20.41 Msi. Similarly, the 1800 °F tests indicated a decrease of 42% and 64% in UTS and failure strain from their corresponding unnotched values. In all of these tests, presence of notch guaranteed a fracture location inside the one inch extensometer gage length. In general, higher temperature did not result in a significant change in material response of notched specimens. The most noticeable differences were occurred in UTS, PLS and its corresponding strain in which temperature resulted in an increase of 8%, 12% and 17% from their corresponding room temperature values respectively.

Table 5: Quasi-static tensile test results of center notched $[(0,90)/(0,90)]_{2s}$ laminates.

Specimen I.D.	Test Temp. (°F)	Elastic Modulus (Msi)	PL Stress @ 0.005% offset (ksi)	PL Strain @ 0.005% offset (%)	Ultimate Strength (ksi)	Ultimate Strain (%)	Fracture Location
0007-001-008-01	75	19.33	9.25	0.053	19.55	0.197	IX
0007-001-008-04	75	21.49	10.25	0.055	18.98	0.199	IX
Ave. Value	***75***	***20.41***	***9.75***	***0.054***	***19.27***	***0.198***	------
0007-001-008-02	1800	21.14	11.25	0.063	20.96	0.188	IX
0007-001-009-02	1800	19.10	10.50	0.063	20.75	0.185	IX
Ave. Value	***1800***	***20.12***	***10.88***	***0.063***	***20.86***	***0.187***	------

4. Conclusions and Recommendations

A material testing system, with a dedicated cooling system, capable of conducting long-term durability tests at elevated temperatures (≤ 2200 °F) was developed. For this system a cold gripping system proved to be suitable for high temperature testing of CMCs. Literaure shows tensile material properties of ceramic matrix composites are significantly influenced by the testing temperature and time at temperature. Depending on the constituents of composite, time and temperature may result in structural evolution of composite (i.e. 100 hours at 1800 °F for SiC/SiC system).

Test results of a CMC model material indicates elevated temperature results in significant changes in material properties. For cross-ply laminates a reduction of 16% in stiffness, an increase of 7% in fracture strength and an increase of 62% in fracture strain were observed. For queasy-isotropic laminates these values were 16%, 12%, and 31% respectively. For both laminates increase in temperature did not affect the proportional limit strength however, the strain associated with that increased 16% and 23% for the cross-ply and quasi-isotropic laminates respectively. Increase in the material properties could be due to relief of residual stresses and disappearance of the interface layer. The material was not held long enough at high temperature to allow for formation of SiO_2. Close inspection of fracture surfaces and the amount of fiber pull out should confirm this assessment.

Presence of a notch reduced the room temperature facture strength by 35% and strain to failure by 38%. The effect was more severe for elevated temperature tests. However, for notched specimens the change in test temperature did not influence the material properties thus indicating that any temperature effect was masked by the dominant effect of notch on damage modes and failure mechanisms.

5. References

1. Enabling Propulsion Materials Program, Quarterly Technical Progress Report, Vol.1 Task A-Combustor, FR 22043-7, Contract No. NAS3-26385.
2. R.W. Davidge, "Mechanical Behavior of Ceramics," Cambridge Univ. Press, Cambridge, 79.
3. R.T. Bhatt, and D.R Behrendt, "Reaction-Bonded Si_3N_4 and SiC Matrix Composites," Flight-vehicle materials, structures, and dynamics - Assessment and future directions. Vol. 3 -

Ceramics and ceramic-matrix composites (A92-39852 16-23). New York, American Society of Mechanical Engineers, 1992, p. 101-111.
4. E.L. Courtright, H.C. Graham, A.P. Katz, and R.J. Kerans, “Ultra High Temp. Assessment Study-Ceramic Matrix Composites,” NASA Tech. Report WL-TR-91-4061, Sep. 1992.
5. J. Aveston, and A. Kelly, “Theory of Multi Fracture of Fibrous Composites,” J.Mat.Sci., 1973, (8).
6. Literature Review of Damage Modes and Failure Mechanisms in Ceramic Matrix Composites, Investigation of Damage Accumulation in Model CMC’s, ESM Dept., Virginia Tech for HSCT initiative, Ref. RFQ 693-K959195, Aug, 1993 .
7. K.K. Chawla,”Composite Materials Science and Engineering,” New York:Springer-Verlag, Inc., 1987, page 250.
8. J. Sankar, A.D. Kelkar, and R. Vaidyanathan, “Investigation of Forced and Isothermal Chemical Vapor Infiltrated SiC/SiC Ceramic Matrix Composites,” Final report, Prepared by NCA&T State University, Mechanical Engineering Department, for ORNL (ORNL/Sub/88-SC423/01), Sept. 1993.
9. P.J. Lamicq, G.A. Bernhart, M.M. Dauchier, and J.G. Mace, “SiC/SiC Composite Ceramics,” Am.Ceram.Soc.Bull, 65[2], 336-338, 1986.
10. A. Chulya, J.Z. Gyekenyesi, and J.P. Gyekenyesi, “Failure Mechanisms of 3-D Woven SiC/SiC Composites under Tensile and Flexural Loading at Room and Elevated Temperatures,”Ceram. Eng.Sci.Proc. , 13[7-8], 420-432,1992.
11. J.M. Yang, J.C. Chou, and C.V. Burkland, “High Temperature/High Performance Composites,” Materials Research Society, Pittsburgh, 1988, 163.
12. C.V. Burkland, W.E. Bustamante, R. Klacka, and J.M. Yang, “Whisker-and Fiber-Reinforced Ceramics,” ASM International, Metals Park, 1988, 225.
13. F.K. Ko, “Preform Fiber Architecture for Ceramic-Matrix Composites,” Ceram.Bull., 68[2],1989, 401-414.
14. J.M. Yang, W. Lin, C.J. Shih, W. Kai, S.M. Jeng, and C.V. Burkland, “Mechanical Behavior of Chemical Vapour Infiltration-Processed Two-and Three-Dimensional Nicalon/SiC Composites,” J.Mat.Sci., 26, 2954-2960, 1991.
15. T. Mah, N.L. Hecht, D.E. McCullum, J.R. Hoenigman, H.M. Kim, A.P. Katz, and H.Lipsitt, “ Thermal Stability of SiC Fibers,” J.Mat.Sci., 19[4], 1984, 1191-1201.
16. D.J. Posher, K.C. Goretta, R.S. Hodder, Jr., and R.E. Tressler, “Strengths of Ceramic Fibers at Elevated Temperatures,” J.Am.Ceram.Soc., 72[2], 284-288,1989.
17. T.J. Clark, R.M. Arons, J.B. Stamatoff, and J. Rabe, “Thermal Degradation of Nicalon[1] SiC Fibers,” Ceram.Eng.Sci.Proc., 7[7-8], 1985, 576-588.
18. T. Mah, M.G. Mendiratta, A.P. Katz, and K.S. Mazdiyasni, “Recent Developments in Fibre-Reinforced High Temperature Ceramic Composites,” Am.Ceram.Soc.Bull. ,66[2],1987,304-308
19. Y. Maniette and A. Oberlin, “TEM Characterization of Some Crude or Air Heat-Treated Silicon Carbide Nicalon Fibers,” J.Mat.Sci., 24[9],1989, 3361-3370.
20. R.D. James, R.A. Lowden, and K.L. More, “The Effects of Oxidation and Combustion Environments on the Properties of Nicalon[*]/SiC Composites,” Ceram.Trans., Vol.19, Advanced Composite Materials, Edited by D.Sacks, Westerville, Ohio 1991.
21. M.H. Headinger, D.H. Roach, and D.J. Landini, “High Temperature Fatigue of Ceramic Matrix Composites,” Presented at AeroMat 1994.

22.Measurement of Test System Alignment Under Tensile Loading,HSR/EPM- TSS-001-93, GE Aircraft Engines, 1 Neumann Way, Mail Drop G-50, Cincinnati , OH. 45215-6301.
23. C.G. Larsen, L.E. Johnson, and L.G. Mosiman, “Gripping Techniques and Concerns for Mechanical Testing of Ultra-High Temperature Materials,” MTS Systems Corporation, Materials Testing Division,Eden Prairie,MN.55344 USA.
24. Monotonic Tensile Testing of Ceramic Matrix, Intermetalic Matrix and Metal Matrix Composite Materials, HSR/EPM-D-001-93 Consensus Standard, GE Aircraft Engines, 1 Neumann Way,Mail Drop G-50,Cincinnati, OH.45215-6301.